Scientific Research Publishing

Energy and Power Engineering, 2023, 15, 500-516
https://www.scirp.org/journal/epe
ISSN Online: 1947-3818
ISSN Print: 1949-243X

Numerical Study of Heat Transfer in a Differentially Heated Cavity

Amadou Konfe, Adrien Sanembaye, Alfred Bayala, Sié Kam

Laboratory of Thermal and Renewable Energies, University Joseph Ki-Zerbo, Ouagadougou, Burkina Faso
Email: konfeamadou@gmail.com

How to cite this paper: Konfe, A., Sanembaye, A., Bayala, A. and Kam, S. (2023) Numerical Study of Heat Transfer in a Differentially Heated Cavity. *Energy and Power Engineering*, **15**, 500-516.
https://doi.org/10.4236/epe.2023.1512028

Received: Novemvber 10, 2023
Accepted: December 24, 2023
Published: December 27, 2023

Abstract

Laminar natural convection is studied in a square cavity filled with air whose two vertical sides are subject to a temperature difference, while the other two horizontal sides are adiabatic. The hot and cold wall temperatures are kept constant. We have presented a dynamic and thermal study of pure natural convection for different values of the Rayleigh number. The numerical simulation was carried out for Rayleigh numbers ranging from 10^2, 10^3, …, 10^5 and the Prandtl number is Pr = 0.71. We used the COMSOL Multiphysic 5.1 software, which allows us to simultaneously solve the coupled physical phenomena in a square enclosure containing air under the Boussinesq approximation. For the coupling of natural convection with radiation from radiative surfaces, both horizontal faces are subjected to radiative flux, and the emissivity of the surfaces varies from Ɛ = 0.1 to 0.8. We have seen that a circulation process is involved. The fluid that is subjected to a high temperature near the hot wall rises to the ceiling and the fluid near the cold wall sinks. This movement continues until the fluid reaches thermal equilibrium. In a natural convection-surface radiation coupling, simulation results indicate that radiative exchange decreases as a function of the Rayleigh number. Surface radiation reduces the flow in the cavity.

Keywords

Natural Convection, Square Cavity, Natural Convection, Radiation Coupling

1. Introduction

The phenomenon of natural convection has received intensive attention in recent years, through various scientific applications: boilers, home heating (case of a radiator) and energy conservation and so on. This transfer method has a very wide field of applications. Several more or less complex geometric configurations

have been examined using theoretical, numerical or experimental approaches [1] [2] [3] [4]. The most commonly used methods include finite differences, finite volumes, finite elements, etc.

The rapid evolution of science in recent years has led to significant progress in our understanding of the phenomena of natural convection, thermal radiation and the coupling of these two phenomena. Given the importance of natural convection in many industrial applications, much previous research has focused on the case of natural convection in regular-shaped enclosures. Studies of natural convection in an enclosure and its coupling with radiation have been carried out by several researchers [5]-[11].

Valencia [4] and Vahl Davis [12] presented a numerical solution of natural convection in a differentially heated square cavity, where the top and bottom surfaces are adiabatic, while the vertical surfaces are heated differently. Ganzarolli and Milanez [11] studied natural convection in rectangular enclosures heated from below and symmetrically cooled from the sides. They varied the Rayleigh number from 10^3 to 10^7 and the aspect ratio from 1 to 9. The influences of Rayleigh number, Prandtl number and aspect ratio on fluid motion and energy transport were presented in their study. Mezrhab and Naji [13] studied a hybrid numerical scheme to simulate the interaction between natural convection and surface radiation in a rectangular, differentially heated cavity. G. Scarella, *et al.* [14] have proposed a study of the interaction between natural convection and radiation for the low Mach approximation for transparent and semi-transparent media. The Navier-stokes and energy equations written for a perfect gas are solved using the finite volume method. The radiation transfer equation is solved by the discrete ordinate method. Wang *et al.* [15] have developed a numerical code for coupling natural convection in a cavity with surface thermal radiation, and studies are being carried out for a cavity filled with air whose four walls have the same emissivity.

Their code is validated by comparing it with data in the literature.

They reveal the lack of precise data for this purpose.

Zhang *et al.* [16] have simulated the coupled natural convection inside and outside a closed cylindrical cavity with a uniform temperature heat source in the center of the cavity in order to understand the influences of Rayleigh number, geometric dimensions of closed cylindrical cavity and cylindrical heat source.

The results indicate that the secondary vortex will appear in the closed cavity with the increasing dimensionless height of the internal heat source and the aspect ratio of the closed cavity.

Among the studies done on cavities of simple geometry, Colomer *et al.* [17] carried out 3D simulations and Velusamy *et al.* [18] studied the interaction of turbulent natural convection with surface radiation (2D k-ε modeling). These studies illustrate the excessive dispersion of the configurations and methodologies used, and the lack of data to validate calculation codes in simple configurations is obvious.

In contrast to pure natural convection in cavities, there is little data on the coupling of natural convection and surface radiation for code validation purposes [15]. The most appropriate configuration seems to be that studied by Akiyama and Chong [19]: A square cavity filled with air, whose four walls have the same emissivity. It should be noted, however, that Akiyama and Chong used an approximate method for calculating the radiation.

In order to enrich the database on natural convection/radiation coupling and understand the effect of radiation on natural convection, a 2D numerical code is implemented in the present paper using COMSOL Multiphysics software.

This allows us to simultaneously solve the coupled physical phenomena in a square enclosure containing air under the Boussinesq approximation. The two vertical walls are differentially heated. On the other hand, the two horizontal walls are either adiabatic (the case of pure natural convection) or subject to radiative conditions, hence the coupling phenomenon.

Most studies in the literature deal with radiative flux, isotherms and Nusselt number as a function of Rayleigh number [5] [6] [9] [11] [12] [15] [20] [21].

This study deals with the temperature distribution, isotherm and velocity in the cavity, taking into account the coupling between convection and radiation.

2. Physical and Mathematical Formulation

2.1. The Natural Convection Differentially Heated Cavity

We retain this study, generally when we submit vertical walls of a cavity filled with air at a constant temperature difference; the flow generated depends on several parameters, the main ones:

- Rayleigh number $R_{aH} = \frac{g\beta\Delta TH^3}{\alpha\upsilon}$.
- Prandtl number $P_r = \frac{\upsilon}{\alpha}$.
- Vertical aspect ratio $A_\upsilon = \frac{H}{l}$.

2.2. Mathematical Formulation

In this configuration, the horizontal walls are adiabatic and the two vertical others are differentially heated. The flow is then monocellular with the upward fluid along the hot wall and descending following the cold wall. We take air as fluid convection within this square cavity.

The two horizontal surfaces are subjected to a radiation flux and taking into account the values used by Wang *et al.* [15] as shown in **Figure 1**. The other faces are vertical to a temperature deviation.

- The hypothesis:
- ✓ The fluid is Newtonian and incompressible.
- ✓ The interior walls are considered gray, diffuse, opaque, and have the same emissivity value Ɛ and Lambertien (emission and reflection with an isotropic luminance).

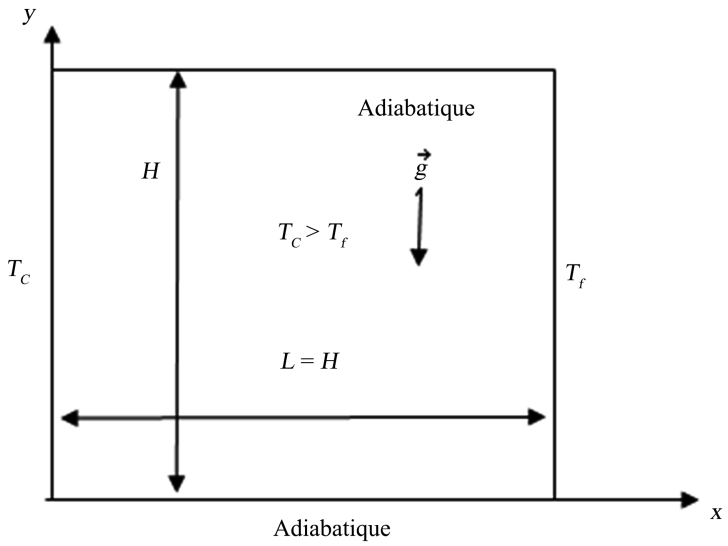

Figure 1. Diagram showing convection in a cavity with a horizontal temperature gradient.

- ✓ The flux densities and temperatures elementary surfaces are uniform.
- ✓ The cavity is filled with a transparent fluid (air), homogeneous and isotropic whose refractive index is equal to unity.
- ✓ The air movement is governed by Navier-Stokes equations under the assumption of Boussinesq.

The equations in Cartesian coordinates are given taking into account the assumptions listed above.

- Continuity equation:

$$\frac{\partial U}{\partial X}+\frac{\partial V}{\partial Y}=0 \tag{1}$$

- Conservation equation for momentum:

Along the x axis: the mass forces are zero, so:

$$\frac{\partial U}{\partial t}+U\frac{\partial U}{\partial X}+V\frac{\partial V}{\partial Y}=\upsilon\left(\frac{\partial^2 U}{\partial X^2}+\frac{\partial^2 U}{\partial Y^2}\right)-\frac{1}{\rho_0}\frac{\partial P}{\partial X} \tag{2}$$

Along the y axis: Due to buoyancy in natural convection;

$$\dot{\rho}=\rho_0-\rho$$

$$\frac{\mathrm{d}V}{\mathrm{d}t}=\left(\rho_0-\rho\right)g+\mu\Delta V-\frac{\partial P}{\partial Y} \tag{3}$$

In natural convection, the density of the fluid ρ_0 is variable, if we use the Boussinesq approximation, $\rho=\rho_0\left(1-\beta\left(T-T_0\right)\right)$ assuming that ρ remains constant in the other terms such as, $\rho=\rho_0$ then we get:

$$\frac{\mathrm{d}V}{\mathrm{d}t}+U\frac{\partial U}{\partial X}+V\frac{\partial V}{\partial Y}=g\beta\left(T-T_0\right)+\upsilon\left(\frac{\partial^2 V}{\partial X^2}+\frac{\partial^2 V}{\partial Y^2}\right)-\frac{1}{\rho_0}\frac{\partial P}{\partial Y} \tag{4}$$

with β the coefficient of thermal expansion.

- Energy conservation equation:

For a two-dimensional system (0, *x*, *y*): $div\left(\overrightarrow{gradT}\right)=\left(\frac{\partial^2 T}{\partial X^2}+\frac{\partial^2 T}{\partial Y^2}\right)$ and $a=\frac{\lambda}{\rho C_{tp}}$ is the thermal diffusivity.

So the equation becomes:

$$\frac{\partial T}{\partial t}+U\frac{\partial T}{\partial X}+V\frac{\partial T}{\partial Y}=a\left(\frac{\partial^2 T}{\partial X^2}+\frac{\partial^2 T}{\partial Y^2}\right) \tag{5}$$

2.3. Choice of Initial and Boundary Conditions

Initial Condition at $t=0, U=0, V=0, T(0,X,Y)=T_0$.

- We assume a non-slip condition to the fluid particles on the walls of the rigid and impermeable pregnant, so that:

$$\begin{cases} U(X=0,Y)=V(X=0,Y)=0 \\ U(X=L,Y)=tV(X=L,Y)=0 \\ U(X,Y=0)=V(X,Y=0)=0 \\ U(X,Y=H)=V(X,Y=H)=0 \end{cases} \tag{6}$$

- With regard to the condition of stationarity of hot and cold temperatures on vertical walls, the following applies:

$$\begin{cases} T=T_C \quad \text{for } X=0,\ 0\le Y\le H \\ T=T_f \quad \text{for } X=L,\ 0\le Y\le H \end{cases} \tag{7}$$

- For horizontal adiabatic walls, the following applies: $\frac{\partial T}{\partial Y}_{/Y=0,H}=0$.

2.4. Scaling the Equations

Dimensioning equations involves making equations dimensionless by using reduced variables.

Let's reduce these equations to dimensionless form. To do this, let's define the characteristic quantities as:

$$\begin{aligned} \frac{\partial u}{\partial \tau}+u\frac{\partial u}{\partial x}+v\frac{\partial u}{\partial y} &= \frac{1}{\rho_0}\sqrt{\frac{P_r}{R_a}}\left(\frac{\partial^2 u}{\partial x^2}+\frac{\partial^2 u}{\partial y^2}\right)-\frac{\partial P}{\partial x}\frac{\partial v}{\partial \tau}+u\frac{\partial v}{\partial x}+v\frac{\partial v}{\partial y} \\ &= \theta+\frac{1}{\rho_0}\sqrt{\frac{P_r}{R_a}}\left(\frac{\partial^2 \upsilon}{\partial x^2}+\frac{\partial^2 \upsilon}{\partial y^2}\right)-\frac{\partial P}{\partial y} \end{aligned} \tag{8}$$

- The energy equation:

$$\frac{\partial T}{\partial t}+U\frac{\partial T}{\partial X}+V\frac{\partial T}{\partial Y}=\frac{\Delta T}{\sqrt{R_a P_r}}\left(\frac{\partial^2 T}{\partial X^2}+\frac{\partial^2 T}{\partial Y^2}\right) \tag{9}$$

2.5. Scaling of Boundary Conditions

- At the initial instant, $\tau=0, \theta(x,y,0)=0$.
- For the temperature on the boundaries of the physical domain:

$$\begin{cases}\theta = 0 & \text{for } x = 0\,;\, 0 \le y \le H \\ \theta = 1 & \text{for } x = L\,;\, 0 \le y \le H\end{cases}.$$

- Whereas for adiabatic wall $\left.\frac{\partial \theta}{\partial y}\right|_{/y=0,1} = 0$.

The theoretical analysis undertaken has made it possible to reduce the number of variables, and to demonstrate that the system to be solved is a function of two main quantities: the Prandtl number Pr and the Rayleigh number Ra.

2.6. Convection-Coupled with Radiation

In the presence of radiation and for a semi-transparent medium, the adiabatic condition is expressed by the equilibrium between convective and radiative fluxes. The coupling of natural convection with surface radiation occurs solely through the thermal boundary conditions. For the two horizontal walls of the cavity, we have:

$$\lambda \left.\frac{\partial T}{\partial y}\right|_{/y=0} - \varphi_{r/y=0} = 0 \tag{11}$$

$$\left.\frac{\partial T}{\partial y}\right|_{/y=H} - \varphi_{r/y=H} = 0 \tag{12}$$

λ is the thermal conductivity of air.

Dimensionless governing equations.

To scale the conservation equations, we will use the same reference quantities as those used for pure natural convection. The reference quantities are the same.

- Dimensioning boundary conditions:

$$\theta = \frac{T - T_0}{T_C - T_f},\quad Q_r = \frac{\varphi_r}{\sigma T_0^4},\quad y = \frac{Y}{H},\quad \Delta T = T_C - T_f,\quad T_0 = \frac{T_C + T_f}{2}.$$

For $y = 0$, we have:

$$-\lambda \left.\frac{\partial T}{\partial y}\right|_{y=0} - \varphi_r = 0 \;\Rightarrow\; \lambda \frac{\partial T}{\partial y} = -\varphi_r,$$

$$\lambda \Delta T \frac{\partial \theta}{H \partial y} = \varphi_r \sigma T_0^4 \;\Rightarrow\; \frac{\partial \theta}{\partial y} = \frac{H}{\lambda \Delta T} \varphi_r \sigma T_0^4 \tag{13}$$

$$\frac{\partial \theta}{\partial y} = N_r Q_r \quad \text{So} \quad N_r = \frac{H \sigma T_0^4}{\lambda \Delta T}.$$

The radiative condition:

$$\lambda \left.\frac{\partial T}{\partial y}\right/_{y=0} = N_r Q_r \tag{14}$$

$$\lambda \left.\frac{\partial T}{\partial y}\right/_{y=1} = -N_r Q_r \tag{15}$$

N_r is the number of radiation ($N_r = \frac{H \sigma T_0^4}{\lambda \Delta T}$).

Q_r is the dimensionless radiative flux $Q_r = \frac{\varphi_r}{\sigma T_0^4}$.

The above equations are to solve using COMSOL software as the simulation tool.

3. Results and Discussions

3.1. Pure Natural Convection

Different velocity and temperature curves were found and compared with those of Hong Wang *et al.* [7].

We investigate the evolution of temperature and vorticity as a function of time at Ra = 10^3 at different positions in the cavity. (x = 0.04; y = 0.04), (x = 0.2; y = 0.2), (x = 0.4; y = 0.4).

Figure 2 above shows different temperature fields as a function of the Rayleigh number in the differentially heated cavity. The two horizontal sides are adiabatic and the other two vertical sides are at T_c = 298.5˚K and T_f = 288.5˚K. A high temperature is seen close to the hot wall and as the temperature increases, it is distributed towards the middle of the cavity, before dropping to a low.

Figure 2 shows the evolution of the temperature as a function of time at different selected points in the cavity. It can be seen that, close to the active wall at a hot temperature, the fluids undergo very significant variations (x = 0.04; y = 0.04) in temperature. At the point (x = 0.4; y = 0.4), these variations become progressively smaller. The dynamic behavior varies with time before reaching an asymptotic limit.

Figure 3 shows the temperature profiles as a function of x for different values of Ra. The temperature distribution is linear for Ra = 10^3, and a strong temperature gradient in the vicinity of the isothermal faces is observed as Ra increases.

Figure 4 and Figure 5 show the temperatures near the upper wall and the lower wall respectively. When the fluid first comes into contact with the hot wall, the hot air rises. There is a high level of heat exchange but as the fluid moves along the high adiabatic wall, it cools. Figure 6 shows that the air cooled by the altitude flows back down towards the low adiabatic wall.

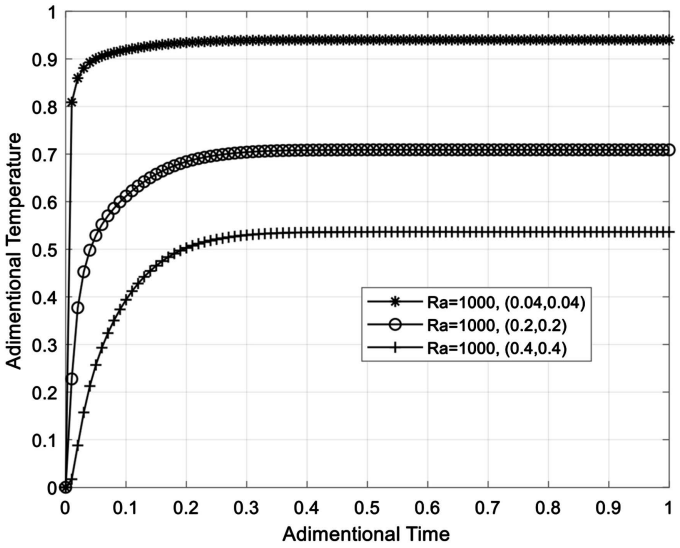

Figure 2. Temperature variation at different positions of x and y for Ra = 10^3.

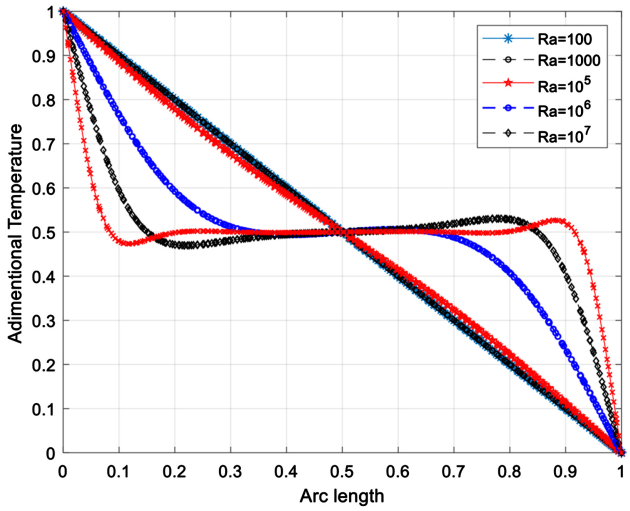

Figure 3. Temperature for different values of Ra.

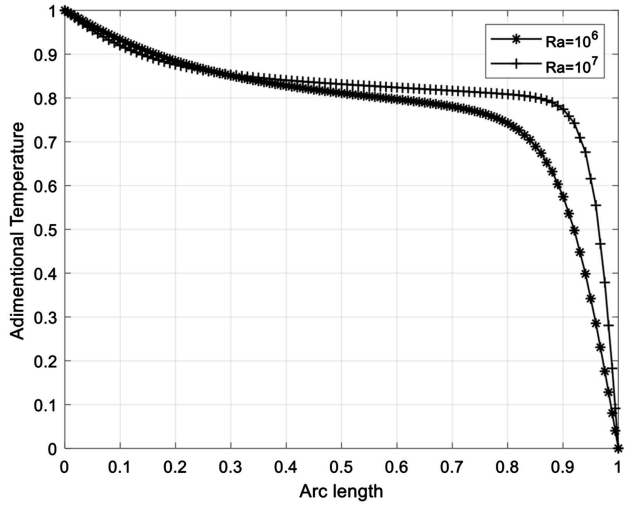

Figure 4. Temperature of the upper wall R = 10^6 and 10^7.

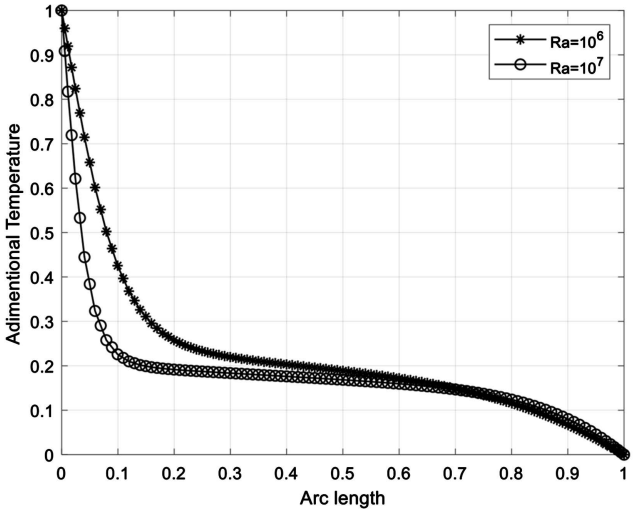

Figure 5. Lower wall temperature R = 10^6 and 10^7.

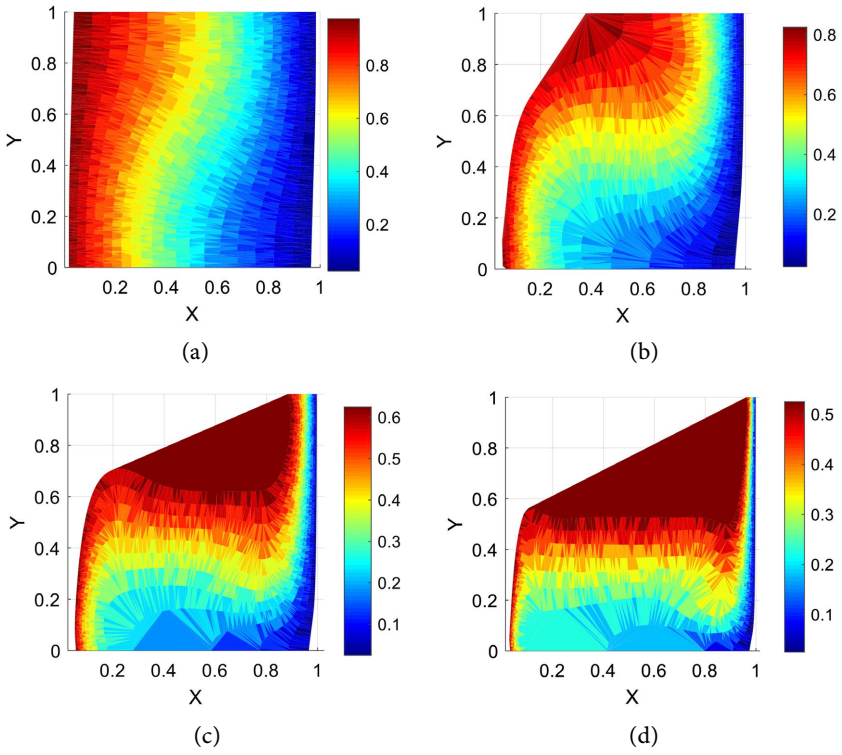

Figure 6. Isotherms for different Ra numbers. (a) Ra = 10^3; (b) Ra = 10^4; (c) Ra = 10^5; (d) Ra = 10^6.

Figure 6 shows the isotherms of the temperature for different values of the Rayleigh number. It shows that for a low value of the Rayleigh number, the fluid (air) exhibits vertical thermal stratification due to heat transfer solely by conduction which does not generate any convective flow. From the result shown in this figure, we can see that the energy transfer for $0 < x < 1$ is one-dimensional. This can be explained by the fact that the isotherms are perpendicular to the main direction of heat transfer, the ox direction. For Ra > 10^3, the isotherms are distorted and contract at the vertical interfaces, mainly due to the relatively high Rayleigh number Ra = 10^7, and the steep temperature gradient at this interface.

Figure 7 shows the evolution of the velocity at different positions for Ra = 10^3. It can be seen that close to the hot wall, the fluid particles have a low velocity (x = 0.04; y = 0.04) but as they move towards the hot wall, the fluids have a high velocity and then this velocity stabilises and takes a horizontal direction.

Figure 8, which shows a velocity field in the cavity for different values of Ra, shows that near the hot wall, the fluid subjected to a high temperature becomes light and therefore moves upwards towards the ceiling, whereas near the cold wall and in the presence of gravity, the fluid close to this wall and therefore heavy, moves downwards towards the low adiabatic wall (floor). This movement continues until the fluid reaches thermal equilibrium.

3.2. Convection Coupled with Radiation

The temperature profile in the case without radiation $\varepsilon = 0$ and in the case with

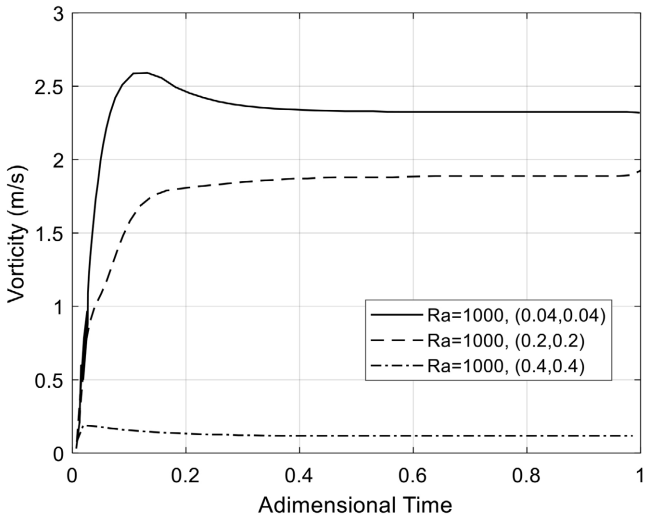

Figure 7. Change in speed at different positions for.

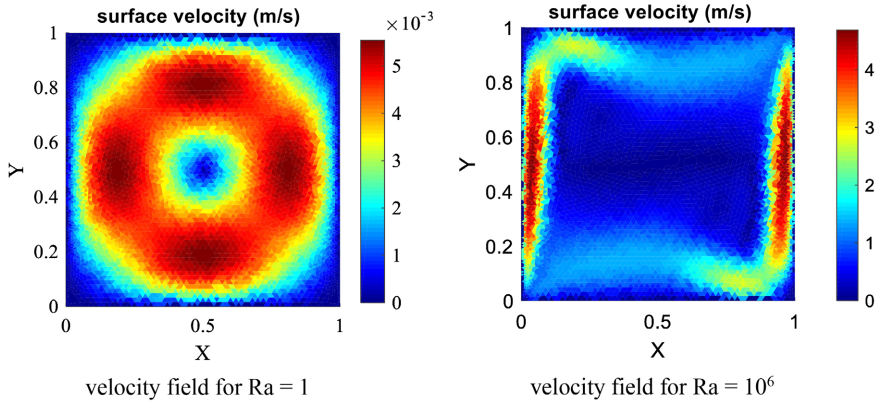

velocity field for Ra = 1 velocity field for Ra = 10^6

Figure 8. Velocity field for different values of Ra.

radiation Ɛ = 0.2 for Ra = 10^4, the influence of emissivity on the isotherms by varying the Rayleigh number Ra and Ɛ = 0; 0.1; 0.2; 0.3; 0.8.

Analysis of this curve (**Figure 9**) shows that when the emissivity of the surfaces is increased, the temperature decreases along the cavity. **Figure 9** shows that for Ra = 10^4, the influence of surface radiation on thermal stratification decreases as a function of emissivity.

In **Figure 10**, the emissivity of the surfaces does not modify the temperature of the upper and lower walls. This can be explained by the fact that the upper wall loses heat (essentially negative net radiative flux) and the lower wall receives heat (essentially positive net radiative flux). Qualitatively speaking, surface radiation has the effect of inducing a flow structure that more closely resembles that in a cavity with perfectly conducting horizontal walls.

According to the analysis of **Figure 11** of the velocity field, the increase in the Rayleigh number leads to an acceleration in the velocity of the flow close to the horizontal and vertical walls and at the centre of the cavity (in blue). By observing the velocity field for Ra = 10^4 and Ɛ = 0.1; Ɛ = 0.2 respectively (b), (d), or for

Ra = 10^5 and Ɛ = 0.1; Ɛ = 0.6 respectively (c), (e), we can see that the variation in emissivity does not modify the velocity of the flow and therefore does not influence the dynamic behavior of the flow.

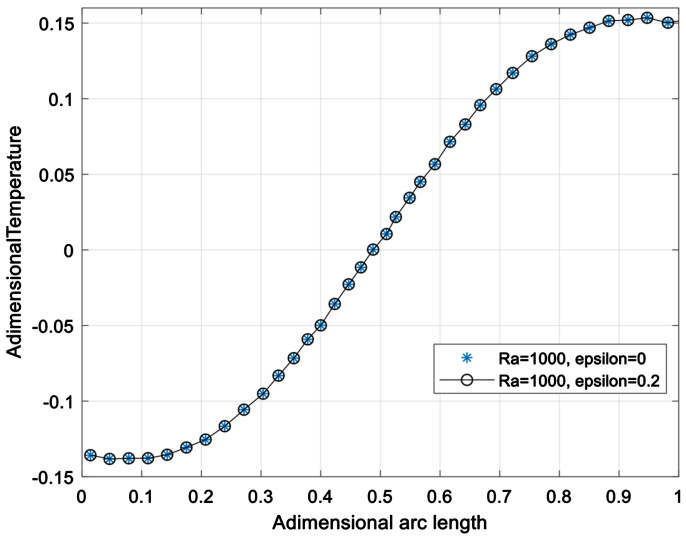

Figure 9. Temperature for Ra = 10^4 and $\varepsilon = 0$, $\varepsilon = 0.2$.

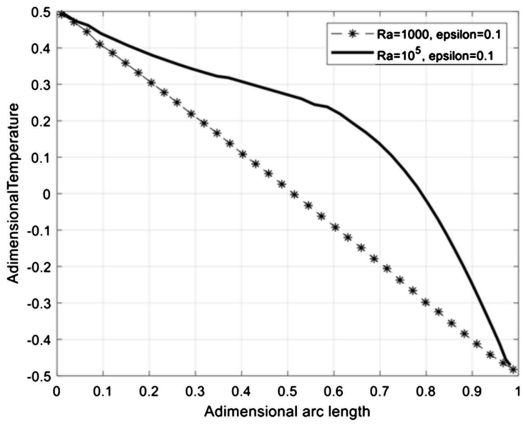

High wall Ra = 10^3 , 10^5 and Ɛ = 0.1

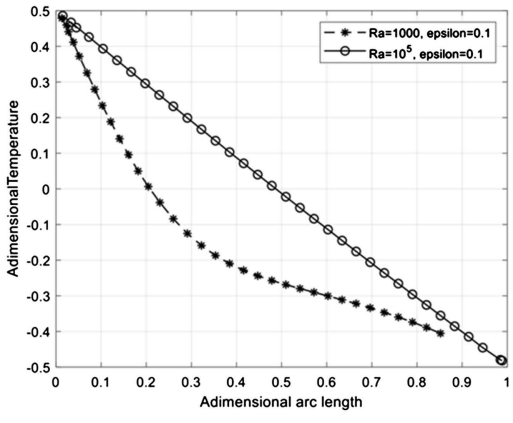

Low wall Ra = 10^3 , 10^5 and Ɛ = 0.1

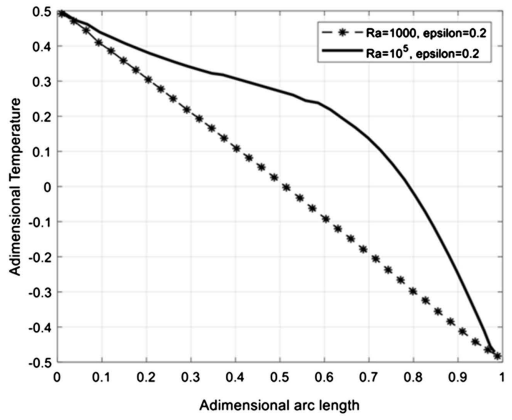

High wall Ra = 10^3 , 10^5 and Ɛ = 0.2

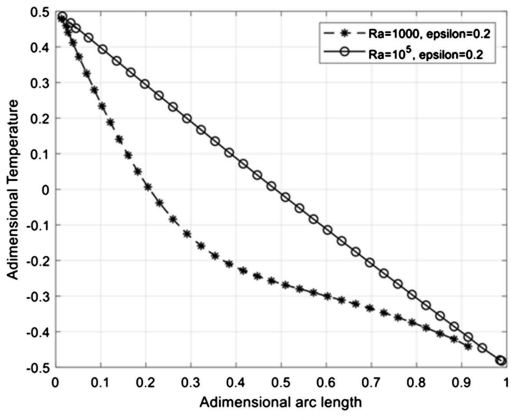

Low wall Ra = 10^3 , 10^5 and Ɛ = 0.2

Figure 10. Upper and lower wall temperatures for Ra = 10^3; 10^5 and $\varepsilon = 0$, $\varepsilon = 0.2$; $\varepsilon = 0.3$.

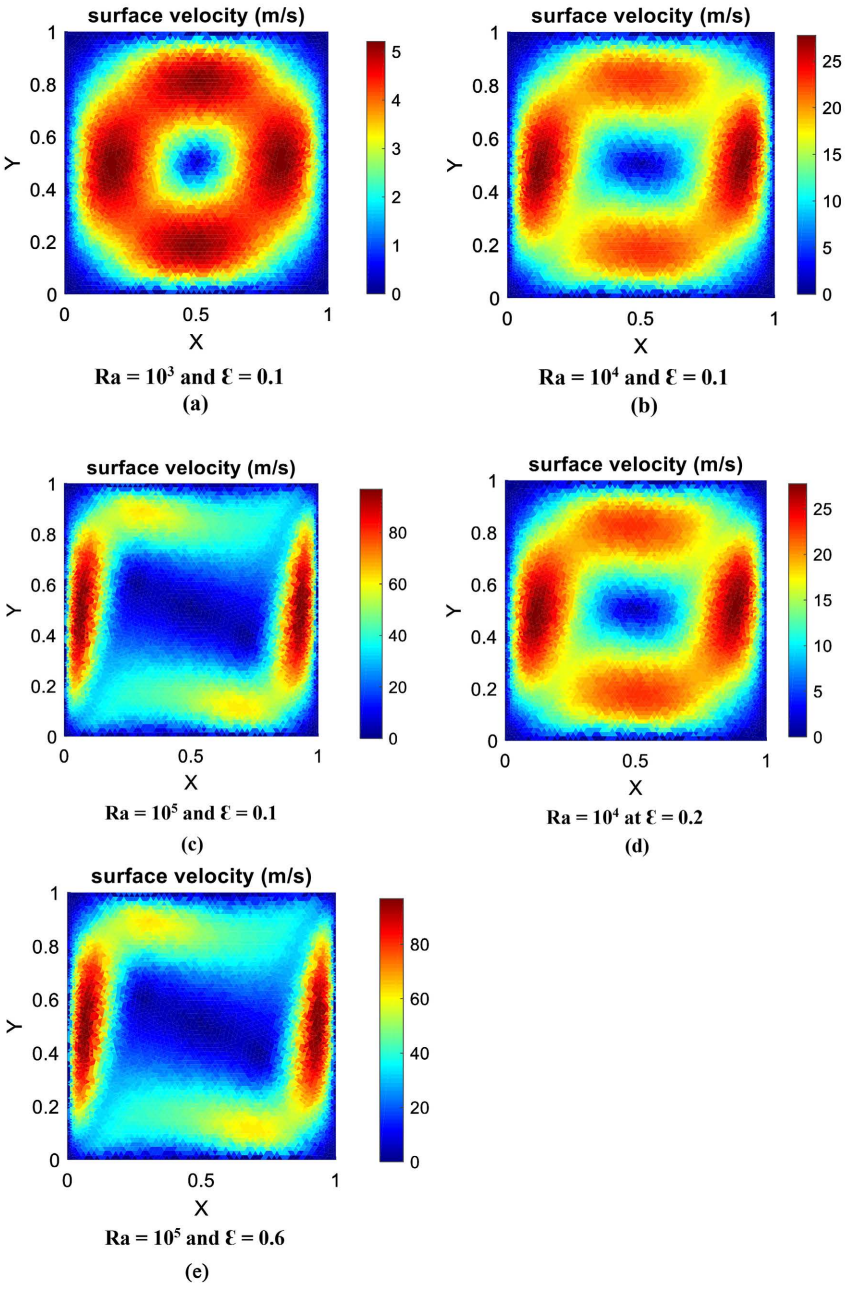

Figure 11. Velocity surface for different values of Ra and $\varepsilon = 0$; $\varepsilon = 0, 2$; $\varepsilon = 0.6$.

Figure 12 shows horizontal velocities as a function of y at different values of Ra (10^3, 10^4, 10^5) and with emissivity Ɛ = 0.1. The velocity profiles indicate a strong acceleration near the horizontal walls, the negative velocities observed over half the cavity ($y < 0$) are characteristic of the recirculation zone. It can be seen that particle velocity increases with increasing Rayleigh number.

4. Code Validation

As announced by Hong *et al.* [15], there is little data on the coupling of natural convection and surface radiation to validate a code.

In addition to the lack of experimental devices to validate our model, validation consists of comparing literature data with our results.

This comparison can only be qualitative given the different simulation conditions.

The Figure 13 shows high and low wall temperatures obtained by Wang *et al.*

We observe a good agreement with those of our simulation.

Figure 14 show the vertical velocity profiles along the horizontal midplanes obtain by Yücef *et al.* [2]. When radiation is not accounted for, the inner core is rather stagnant. Radiation causes an overall increase in the velocities.

Large velocity gradients exist along both the thermally active and insulated walls.

Similar results are obtain by Kane *et al.* [7] as show in Figure 15.

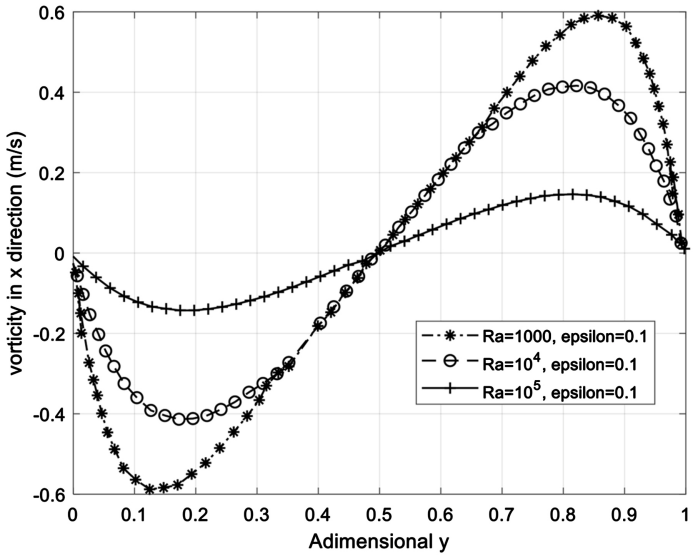

Figure 12. Velocity curves along y at different values of Ra and $\varepsilon = 0.1$.

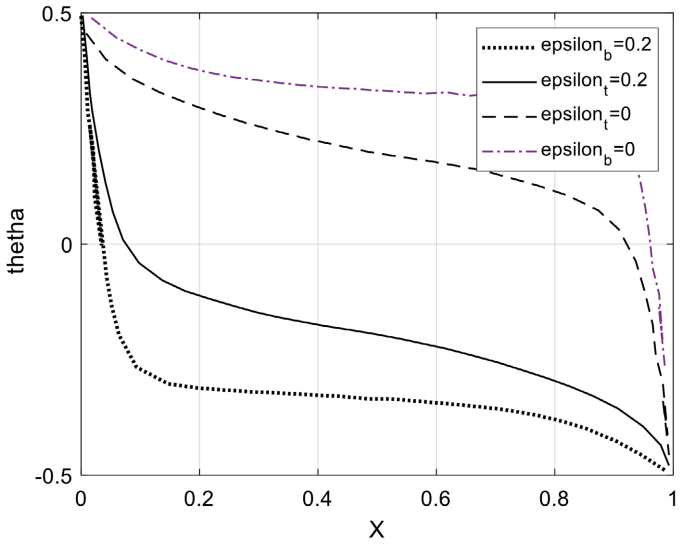

Figure 13. Temperature on the horizontal walls at Ra = 10^6 [15].

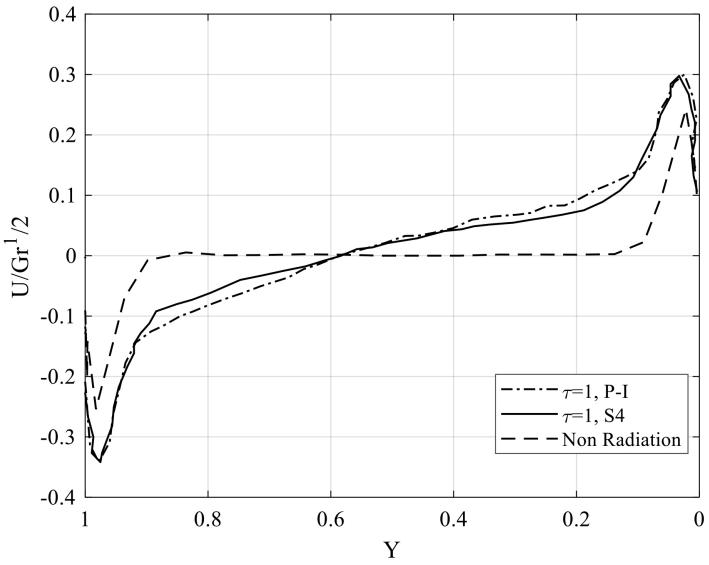

Figure 14. Vertical velocity profiles for radiating fluid on X = 0.5 midplane. Ra_E (external Rayleigh number) = 5×10^6. Ra_i (internal Rayleigh number) = 0, Pl (planck number) = 0.02., w (scattering albedo) = 0 [2].

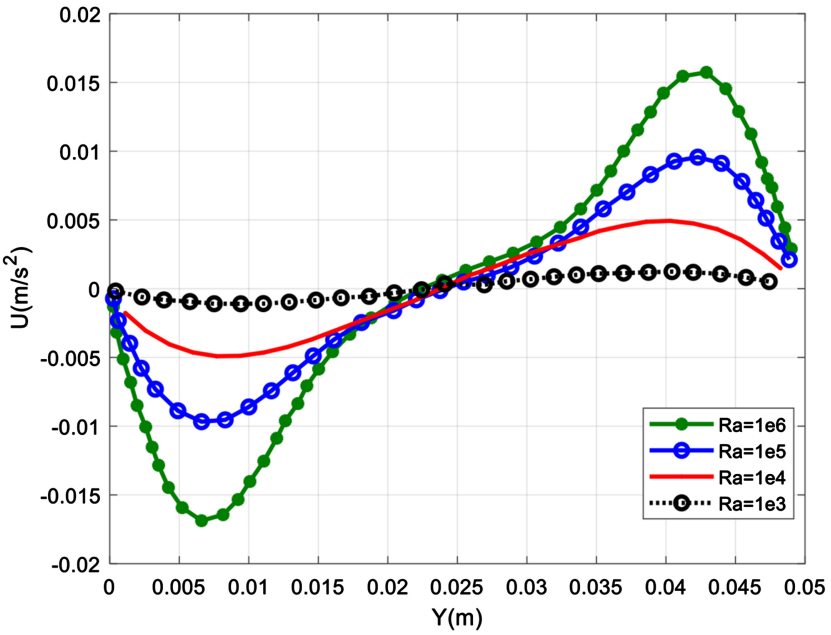

Figure 15. Variation of horizontal velocity at mid-cavity (vertical line) for different rayleigh numbers [7].

It is observed that the amplitudes of velocities increased in the vicinity of the heated left wall by being canceled towards $x = 0.025$ m and decreasing near the active right wall.

Their study concludes that the velocity increase with the increase of the Rayleigh number.

These qualitatives comparison allowed us to validate les results of our simulation.

5. Conclusions

In this paper, we studied pure natural convection, the process of thermal radiation and the coupling of natural convection with radiation from radiating surfaces. In pure natural convection, the cavity is differentially heated on its two vertical faces, but in coupling, the two horizontal faces are subjected to a radiative flux.

We have presented a dynamic and thermal study of pure natural convection for different values of the Rayleigh number. The numerical simulation was carried out for Rayleigh numbers ranging from 10^2, 10^3, …, 10^5. It was found that a circulation process is involved. The fluid subjected to a high temperature near the hot wall rises to the ceiling and the fluid near the cold wall sinks. This movement continues until the fluid reaches thermal equilibrium.

Based on the results, the following conclusions are drawn:

- Variation in emissivity does not modify the velocity of the flow and therefore does not affect the dynamic behaviour of the flow.
- Particle velocity increases with increasing Rayleigh number.
- An increase in surface emissivity does not influence the isotherms.
- The emissivity of the surfaces does not modify the temperature of the upper and lower walls.
- The influence of surface radiation on thermal stratification decreases as a function of emissivity.

As a suggestion for future works, the transient regime can be studied, as well as fluid properties varying with temperature, the utilization of participating media sources and other geometries.

Acknowledgements

We gratefully acknowledge the ISP, Uppsala University, Sweden for their support to project BUF01.

Conflicts of Interest

The authors declare no conflicts of interest regarding the publication of this paper.

References

[1] Rashid, F.L., *et al.* (2023) Analysis of Heat Transfer in Various Cavity Geometries with and without Nano-Enhanced Phase Change Material: A Review. *Energy Reports*, **10**, 3757-3779. https://doi.org/10.1016/j.egyr.2023.10.036

[2] Yücel, A., Acharya, S. and Williams, M.L. (1989) Natural Convection and Radiation in a Square Enclosure. *Numerical Heat Transfer*, *Part A*: *Applications*, **15**, 261-278. https://doi.org/10.1080/10407788908944688

[3] Yan, G., *et al.* (2023) Natural Convection of Rectangular Cavity Enhanced by Obstacle and Fin to Simulate Phase Change Material Melting Process Using Lattice Boltzmann Method. *Alexandria Engineering Journal*, **81**, 319-336. https://doi.org/10.1016/j.aej.2023.09.035

[4] Valencia, A. and Frederick, R.L. (1989) Heat Transfer in Square Cavities with Partially Active Vertical Walls. *International Journal of Heat and Mass Transfer*, **32**, 1567-1574. https://doi.org/10.1016/0017-9310(89)90078-1

[5] Kishor, V., Singh, S. and Srivastava, A. (2018) Investigation of Convective Heat Transfer Phenomena in Differentially-Heated Vertical Closed Cavity: Whole Field Experiments and Numerical Simulations. *Experimental Thermal and Fluid Science*, **99**, 71-84. https://doi.org/10.1016/j.expthermflusci.2018.07.021

[6] Khatamifar, M., Lin, W. and Dong, L. (2021) Transient Conjugate Natural Convection Heat Transfer in a Differentially-Heated Square Cavity with a Partition of Finite Thickness and Thermal Conductivity. *Case Studies in Thermal Engineering*, **25**, Article ID: 100952. https://doi.org/10.1016/j.csite.2021.100952

[7] Kane, M.K., Mbow, C., Sow, M.L. and Sarr, J. (2017) A Study on Natural Convection of Air in a Square Cavity with Partially Thermally Active Side Walls. *OJFD*, **7**, 623-641. https://doi.org/10.4236/ojfd.2017.74041

[8] Ibrahim, A., Saury, D. and Lemonnier, D. (2013) Coupling of Turbulent Natural Convection with Radiation in an Air-Filled Differentially-Heated Cavity at Ra = 1.5 Â 109. *Computers & Fluids*, **88**, 115-125. https://doi.org/10.1016/j.compfluid.2013.09.006

[9] Hernández-Castillo, P., Castillo, J.A. and Huelsz, G. (2022) Heat Transfer by Natural Convection and Radiation in Three Dimensional Differentially Heated Tall Cavities. *Case Studies in Thermal Engineering*, **40**, Article ID: 102529. https://doi.org/10.1016/j.csite.2022.102529

[10] Greenspan, D. and Schultz, D. (1974) Natural Convection in an Enclosure with Localized Heating from below. *Computer Methods in Applied Mechanics and Engineering*, **3**, 1-10. https://doi.org/10.1016/0045-7825(74)90038-3

[11] Ganzarolli, M.M. and Milanez, L.F. (1995) Natural Convection in Rectangular Enclosures Heated from below and Symmetrically Cooled from the Sides. *International Journal of Heat and Mass Transfer*, **38**, 1063-1073. https://doi.org/10.1016/0017-9310(94)00217-J

[12] De Vahl Davis, G. (1983) Natural Convection of Air in a Square Cavity: A Bench Mark Numerical Solution. *Numerical Methods in Fluids*, **3**, 249-264. https://doi.org/10.1002/fld.1650030305

[13] Mezrhab, A. and Naji, H. (2009) Coupling of Lattice Boltzmann Equation and Finite Volume Method to Simulate Heat Transfer in a Square Cavity. *Fluid Dynamic and Material Process*, **5**, 283-295

[14] Scarella, G., Accary, G., Meradji, S., Morvan, D. and Bessonov, O.A. (2008) Three-Dimensional Numerical Simulation of the Interaction between Natural Convection and Radiation in a Differentially Heated Cavity in the Low Mach Number Approximation. In: *International Symposium on Advances in Computational Heat Transfer*, Marrakesh, Begell House, Morocco, 1-8. https://doi.org/10.1615/ICHMT.2008.CHT.740

[15] Wang, H., Xin, S. and Le Quéré, P. (2006) Étude numérique du couplage de la convection naturelle avec le rayonnement de surfaces en cavité carrée remplie d'air. *Comptes Rendus Mécanique*, **334**, 48-57. https://doi.org/10.1016/j.crme.2005.10.011

[16] Zhang, L., Chen, C. and Li, Y.-R. (2023) Coupled Natural Convection Heat Transfer inside and outside a Closed Cylindrical Cavity with a Uniform Temperature Heat Source. *Case Studies in Thermal Engineering*, **52**, Article ID: 103659. https://doi.org/10.1016/j.csite.2023.103659

[17] Colomer, G., Costa, M., Cònsul, R. and Oliva, A. (2004) Three-Dimensional Numeri-

cal Simulation of Convection and Radiation in a Differentially Heated Cavity Using the Discrete Ordinates Method. *International Journal of Heat and Mass Transfer*, **47**, 257-269. https://doi.org/10.1016/S0017-9310(03)00387-9

[18] Velusamy, K., Sundararajan, T. and Seetharamu, K.N. (2001) Interaction Effects between Surface Radiation and Turbulent Natural Convection in Square and Rectangular Enclosures. *Journal of Heat Transfer*, **123**, 1062-1070. https://doi.org/10.1115/1.1409259

[19] Akiyama, M. and Chong, Q.P. (1997) Numerical Analysis of Natural Convection with Surface Radiation in a Square Enclosure. *Numerical Heat Transfer*, *Part A*: *Applications*, **32**, 419-433. https://doi.org/10.1080/10407789708913899

[20] Balaji, C. and Venkateshan, S.P. (1993) Interaction of Surface Radiation with Free Convection in a Square Cavity. *International Journal of Heat and Fluid Flow*, **14**, 260-267. https://doi.org/10.1016/0142-727X(93)90057-T

[21] Das, S. and Bhattacharya, P. (2015) Effect of Prandtl Number on Laminar Natural Convective Heat Transfer inside Cavity. *Procedia Engineering*, **127**, 229-234. https://doi.org/10.1016/j.proeng.2015.11.334